

Analiza vezanega prenosa toplote v hladilniku elektronskega čipa

An Analysis of Conjugate Heat Transfer in the Heat Sink of an Electronic Chip

Andrej Horvat - Ivan Catton

Prispevek opisuje razvoj algoritma za izračun vezanega prenosa toplote z namenom izbire najugodnejše geometrijske oblike za hladilnik elektronskega čipa. Struktura hladilnika je bila modelirana kot homogena porozna snov z uporabo teorije prostorninskega povprečenja (TPP - VAT). Geometrijska oblika simulacijskega območja in robni pogoji so bili povzeti po eksperimentalni napravi v laboratoriju za prenos toplote "Morrin-Martinelli-Gier" na Univerzi Kalifornije v Los Angelesu. Primeri numeričnih simulacij so bili izvedeni za izotermno testno sekcijo kakor tudi za topotno prevodno testno sekcijo iz aluminija. Primerjava koeficienta upora celotne proge \bar{C}_d kot funkcije Reynoldsovega števila Re_h razkriva dobro ujemanje z objavljenimi rezultati, medtem ko primerjava porazdelitev Nusseltovega števila \bar{Nu} kaže večje razlike. Končna topotna prevodnost trdnine zmanjša koeficient prestopa toplote in Nusseltovo število \bar{Nu} . Vpliv topotne prevodnosti na rezultate se zvečuje s povečevanjem Reynoldsovega števila.

© 2002 Strojniški vestnik. Vse pravice pridržane.

(Ključne besede: prenosniki toplote, hladilniki čipov, prenos toplote, razvoj algoritmov)

This paper describes the construction of an algorithm for conjugate heat-transfer calculations in order to find the most suitable form for the heat sink of an electronic chip. Applying volume averaging theory (VAT) to a system of transport equations, a heat-sink structure was modeled as a homogeneous porous medium. The geometry of the simulation domain and the boundary conditions followed the experimental set-up used in the Morrin-Martinelli-Gier Memorial Heat Transfer Laboratory at the University of California, Los Angeles. The example numerical simulations were performed for the test section with an isothermal structure as well as for the heat-conducting aluminum pin-fins. A comparison of the whole-section drag coefficient \bar{C}_d as a function of Reynolds number Re_h reveals good agreement with existing data, whereas the comparison of the Nusselt number \bar{Nu} distributions shows larger discrepancies. The finite conductivity of the solid decreases the heat-transfer coefficient and Nusselt number \bar{Nu} . The influence of conductivity becomes larger with increasing Reynolds number.

© 2002 Journal of Mechanical Engineering. All rights reserved.

(Keywords: heat exchangers, heat sinks, heat transfer, algorithms)

0 UVOD

Prenosniki toplote so ena od osnovnih komponent ne samo v termoenergetski in procesni industriji ampak tudi v proizvodnji elektronske opreme. Navkljub pomembni vlogi, je v konstrukcijski postopek prenosnikov toplote še vedno vpleteno mnogo izkustvenih spoznanj. V preteklosti sta se namreč razvoj in uporaba prenosnikov toplote razvijala ločeno na številnih, največkrat nepovezanih področjih, zlasti v avtomobilski in letalski industriji, v kriogeni in hladilniški tehniki. Pri tem so se tehnologije, dobro znane v enem področju, le počasi širile na druga področja [1]. Zaradi tega lahko skupen način izbire in optimizacije konstrukcije prenosnikov toplote pomembno zmanjša stroške v industriji.

0 INTRODUCTION

Heat exchangers are one of the basic installations, not only in power and process industries, but also in the production of electronic equipment. Despite their crucial role, there is still a great deal of empiricism involved in the design procedure of heat exchangers. The development and application of heat exchangers and their surfaces has taken place in a piecemeal fashion in a number of rather unrelated areas, principally those of the automotive, aerospace, cryogenic and refrigeration sectors. A lot of detailed technology, familiar in one sector, progressed only slowly over the boundary into another sector [1]. Therefore, a unifying approach to select and to optimize a heat-exchanger design can bring significant cost reduction to industry.

Prispevek je del širših prizadevanj za razvoj znanstvenega prostopa k problemu optimizacije geometrijske oblike prenosnikov toplotne. Opisuje gradnjo algoritma za hiter izračun vezanega prenosa toplotne z namenom izbiro najugodnejše geometrijske oblike za hladilnik elektronskega čipa.

Struktura hladilnika je bila modelirana kot homogen porozen medij z uporabo teorije prostorninskega povprečenja (TPP) ([2] do [4]) sistema prenosnih enačb. Medsebojni vpliv tekočine in strukture je bil opisan s koeficienti lokalnega upora C_d in prestopa toplotne h , ki so bili prevzeti iz razpoložljive literature ([7] do [9]) in vstavljeni v računalniški program.

Izračunani koeficient upora celotne proge \bar{C}_d , toplotna učinkovitost \bar{Q}/\bar{W} in Nusseltovo število Nu so bili primerjani z razpoložljivimi eksperimentalnimi podatki [5]. Primerjava kaže dobro ujemanje s preskusi kljub poenostavljivosti predstavljenega modela.

1 MODELNI PRISTOP

Zračni tok skozi hladilnik čipa lahko opišemo z osnovnimi enačbami prenosa snovi, gibalne količine in energije [6]. Zaradi zahtev po kratkem računskem času modela, je treba prenosnim enačbam izračunati povprečje po periodični nadzorni prostornini (za podrobnosti glej [4]). To prostorninsko računanje povprečja vodi do problema sklenitve sistema enačb, pri katerem je treba prenos gibalne količine in toplotne med tekočino in trdnino opisati z empiričnimi razmerji, npr. s koeficientoma lokalnega upora C_d in prestopa toplotne h .

Da bi še nadalje poenostavili simuliran sistem, smo predpostavili tok tekočine le v vzdolžni smeri z nespremenljivim znižanjem tlaka (sl. 1). Zaradi tega se profil hitrosti spreminja le prečno na smer toka. To pomeni, da je tlačna sila čez celotno simulacijsko območje v ravnovesju s strižnimi silami. Tako je mogoče enačbo prenosa gibalne količine zapisati v diferencialni obliki kot:

$$-\alpha_f \mu_f \left(\frac{\partial^2 u_f}{\partial y^2} + \frac{\partial^2 u_f}{\partial z^2} \right) + \frac{1}{2} C_d \rho_f u_f^2 S = \frac{\Delta p}{L} \quad (1),$$

kjer so: α_f delež tekočine, C_d koeficient lokalnega upora, S specifična površina porozne snovi, Δp padec tlaka čez simulacijsko območje in L dolžina simulacijskega območja.

Temperaturno polje v tekočini se oblikuje pod vplivom ravnovesja med toplotno konvekcijo v smeri toka, toplotno difuzijo in toplotno, ki se prenese s trdnino na tekočino. Iz tega izhaja diferencialna oblika energijske enačbe za tekočino:

$$\alpha_f \rho_f c_f u_f \frac{\partial T_f}{\partial x} = \alpha_f \lambda_f \left(\frac{\partial^2 T_f}{\partial x^2} + \frac{\partial^2 T_f}{\partial y^2} + \frac{\partial^2 T_f}{\partial z^2} \right) - h (T_f - T_s) S \quad (2),$$

kjer sta: T_f temperatura tekočine in T_s temperatura trdnine. Prenos toplotne med trdnino in tekočino je

This paper is part of a broader effort to develop a scientific procedure for optimization of heat-exchanger geometries. It describes the construction of an algorithm for fast calculations of conjugate heat transfer in order to find the most suitable form for an electronic chip heat sink.

Applying volume averaging theory (VAT) ([2] to [4]) to a system of transport equations, a heat-sink structure was modeled as a homogeneous porous media. The interaction between the fluid and the heat-sink structure was described with local drag and heat-transfer coefficients, which were taken from the available literature ([7] to [9]) and inserted into a computer code.

The calculated whole-section drag coefficient \bar{C}_d , thermal effectiveness \bar{Q}/\bar{W} and Nusselt number Nu were compared with available experimental data [5]. The comparison shows a good agreement with the experimental data despite model simplifications.

1 MODEL APPROACH

The airflow through a chip-cooler structure can be described with basic mass, momentum and heat-transport equations [6]. Due to the requirement for the model to have short computing times, the transport equations have to be averaged over a periodic control volume (see [4] for details). This volumetric averaging leads to a closure problem, where an interface exchange of momentum and heat between a fluid and a solid has to be described with additional empirical relations, e.g. a local drag coefficient C_d and a local heat-transfer coefficient h .

To further simplify the simulated system, fluid flow was taken as unidirectional with a constant pressure drop in the streamwise direction (Fig. 1). As a consequence, velocity only changes transverse to the flow direction. This means that the pressure force across the entire simulation domain is balanced with shear forces. Thus, the momentum equation can be written in differential form as:

$$+\frac{1}{2} C_d \rho_f u_f^2 S = \frac{\Delta p}{L} \quad (1),$$

where α_f is the fluid fraction, C_d the local drag coefficient, S the specific surface of porous media, Δp the pressure drop across the simulation domain and L the simulation domain's length.

The temperature field in the fluid is formed as a balance between thermal convection in the streamwise direction, thermal diffusion, and the heat that is transferred from the solid to the fluid. Thus, the differential form of the energy equation for the fluid is:

$$\alpha_f \rho_f c_f u_f \frac{\partial T_f}{\partial x} = \alpha_f \lambda_f \left(\frac{\partial^2 T_f}{\partial x^2} + \frac{\partial^2 T_f}{\partial y^2} + \frac{\partial^2 T_f}{\partial z^2} \right) - h (T_f - T_s) S \quad (2),$$

where T_f and T_s are the fluid and solid temperatures, respectively. The heat transfer between the solid and the

modeliran kot linearna odvisnost temperatur obih faz, kjer je h koeficient lokalnega prestopa toplotne.

V vsaki nadzorni prostornini je struktura hladilnika le šibko povezana v vodoravni smeri (sl. 1). Zaradi tega je le toplotna difuzija v navpični smeri v ravnovesju s toploto, ki odteka skozi stično površino kapljevine in trdnine, medtem ko lahko toplotno difuzijo v vodoravni smeri zanemarimo. To poenostavi energijsko enačbo trdnine:

$$0 = \alpha_s \lambda_s \frac{\partial^2 T_s}{\partial z^2} + h (T_f - T_s) S \quad (3)$$

kjer je α_s delež trdnine.

Eračbe (1) do (3), ki so zapisane s povprečenimi veličinami, so eračbe ravnovesnega prenosa gibalne količine in toplotne skozi homogeno porozno snov. Zanesljive podatke za dva dodatna parametra, to sta koeficiente lokalnega upora C_d in prestopa toplotne h , smo poiskali v [7] do [9].

fluid is modeled as a linear relation between both phase temperatures, where h is a local heat-transfer coefficient.

The chip-cooler structure in each control volume is only loosely connected in the horizontal directions (see Fig. 1). As a consequence, only the thermal diffusion in a vertical direction is in balance with the heat leaving the structure through the fluid-solid interface, whereas the thermal diffusion in horizontal directions can be neglected. This simplifies the energy equation for the solid to:

$$0 = \alpha_s \lambda_s \frac{\partial^2 T_s}{\partial z^2} + h (T_f - T_s) S \quad (3)$$

where α_s is the solid fraction.

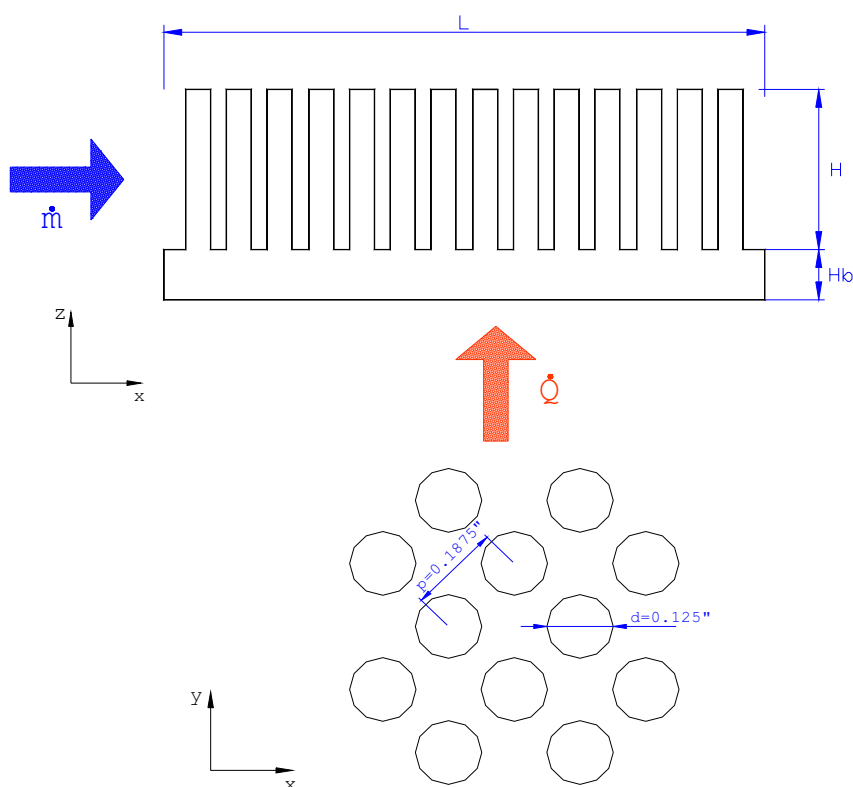
Equations (1) to (3), written with the phase averaged variables, are equations for the steady-state transport of momentum and heat through homogeneous porous media. The reliable empirical data for two additional parameters, a local drag coefficient C_d and heat-transfer coefficient h , were found in [7] to [9].

2 SIMULACIJSKO OBMOČJE

Geometrijska oblika simulacijskega območja kakor tudi robni pogoji enačb (1) do (3) sledijo geometrijski oblik eksperimentalne testne sekcije, ki je bila uporabljena v laboratoriju za prenos toplotne "Morrin-Martinelli-Gier" na Univerzi Kalifornije v Los Angeles za pridobitev eksperimentalnih podatkov, opisanih v [5].

2 SIMULATION DOMAIN

The geometry of the simulation domain as well as the boundary conditions for Eqs. (1-3) follow the geometry of the experimental test section used in the Morrin-Martinelli-Gier Memorial Heat Transfer Laboratory at the University of California, Los Angeles, where the experimental data described in [5] were taken.



Sl. 1. Eksperimentalna testna proga
Fig. 1. Experimental test section

Splošna razporeditev palčnih reber hladilnika je podana na sliki 1. Premer palčnih reber je znašal $d = 0,003175 \text{ m}$ ($0,125''$). Razmerje medpalčnega razmika in premera v smeri toka je bilo $p_x/d = 1,06$ in v smeri prečno na tok $p_y/d = 2,12$. Simulacijsko območje je zajemalo 34 vrst palčnih reber v smeri toka in 17 vrst prečno na smer toka. Dolžina hladilnika L kakor tudi širina W sta znašali $0,1145 \text{ m}$, medtem ko je višina H znašala $0,0381 \text{ m}$.

Robni pogoji trdne stene brez zdrsa so bili uporabljeni za enačbo prenosa gibalne količine (1) na vseh štirih stenah, ki so vzporedne s smerjo toka:

$$u_f(0,z)=0, \quad u_f(W,z)=0, \quad u_f(y,0)=0, \quad u_f(y,H)=0 \quad (4).$$

Kot gonilna sila toka je bil podan tlačni padec vzdolž celotnega simulacijskega območja. Absolutne vrednosti so zbrane v preglednici 1.

Pri enačbi prenosa energije v tekočini (2) smo predpostavili izotermni vtok tekočine kot tudi izotermno spodnjo steno:

$$T_f(0,y,z)=T_{in}, \quad T_f(x,y,0)=T_g \quad (5),$$

medtem ko so bile druge stene adiabatne:

$$\frac{\partial T_f}{\partial x}(L,y,z)=0, \quad \frac{\partial T_f}{\partial y}(x,0,z)=0, \quad \frac{\partial T_f}{\partial y}(x,W,z)=0, \quad \frac{\partial T_f}{\partial z}(x,y,H)=0 \quad (6).$$

Pri enačbi prenosa energije v trdnini (3) je bila spodnja stena privzeta kot izotermna, medtem ko je bila zgornja stena adiabatna:

$$T_s(x,y,0)=T_g, \quad \frac{\partial T_s}{\partial z}(x,y,H)=0 \quad (7).$$

Predpostavka o izotermnosti spodnje stene (5) in (7) se pomembno razlikuje od eksperimentalne postavitve [5], pri kateri so palčna rebra spojena s toplotno prevodno bazno ploščo. Kljub vsemu bodo rezultati pokazali, da sedanji model daje zadovoljiv približek izmerjenih vrednosti.

Absolutne temperature robnih pogojev za različne simulirne primere so zbrane v preglednici 1.

3 NUMERIČNE METODE

Prenosne enačbe (1) do (3) in robni pogoji (4) do (7) so bili preoblikovani v brezdimenzijsko obliko in diskretizirani, upoštevajoč načela metode končnih

Preglednica 1. Robni pogoji - izbrane vrednosti
Table 1. Boundary conditions - pre-set values

Št. No.	$\Delta p \text{ Pa}$	$T_{in} \text{ }^{\circ}\text{C}$	$T_g \text{ }^{\circ}\text{C}$
1	5,0	23,00	54,90
2	10,0	23,00	43,43
3	20,0	23,00	37,20
4	40,0	23,00	33,00

The general arrangement of the heat-sink pin-fins is given in Fig. 1. The diameter of the pin-fins was $d = 0.003175 \text{ m}$ ($0.125''$). The pitch-to-diameter ratio in the streamwise direction was set to $p_x/d = 1.06$, and in the transverse direction to $p_y/d = 2.12$. The simulation domain consisted of 34 rows of pin-fins in the streamwise direction and 17 rows of pin-fins in the transverse direction. The length L as well as the width W of the heat sink were 0.1145 m , whereas the height H was 0.0381 m .

The no-slip boundary conditions for the momentum equation (1) were implemented for all four walls, which are parallel to the flow direction:

$$u_f(0,z)=0, \quad u_f(W,z)=0, \quad u_f(y,0)=0, \quad u_f(y,H)=0 \quad (4).$$

As a flow driving force, the whole-section pressure drop Δp was prescribed. The absolute values are summarized in Table 1.

For the fluid energy equation (2), the simulation domain inflow and the bottom wall were taken as isothermal:

whereas the other walls were considered as adiabatic:

$$\frac{\partial T_f}{\partial x}(L,y,z)=0, \quad \frac{\partial T_f}{\partial y}(x,0,z)=0, \quad \frac{\partial T_f}{\partial y}(x,W,z)=0, \quad \frac{\partial T_f}{\partial z}(x,y,H)=0 \quad (6).$$

For the solid energy equation (3), the bottom wall was prescribed as isothermal, whereas the top wall was assumed to be adiabatic:

$$\frac{\partial T_s}{\partial z}(x,y,H)=0 \quad (7).$$

The assumption about the isothermal bottom wall (5) and (7) significantly differs from the experimental set-up [5], where the pin-fins were joined with a conductive base plate. Nevertheless, as the results will show, the presented model still gives a satisfactory approximation to the measured values.

The absolute temperatures in different simulation cases are summarized in Table 1.

3 NUMERICAL METHODS

The transport equations (1) do (3) and boundary conditions (4) to (7) were transformed into the dimensionless form and then discretized following

Št. No.	$\Delta p \text{ Pa}$	$T_{in} \text{ }^{\circ}\text{C}$	$T_g \text{ }^{\circ}\text{C}$
5	74,7	23,02	30,30
6	175,6	23,02	27,90
7	266,5	23,04	27,30
8	368,6	22,85	26,64

prostornin ([6] in [10]). Pri vseh izvedenih numeričnih simulacijah smo uporabili $34 \times 17 \times 70$ končnih prostornin v smereh x , y in z .

Zaradi robnih pogojev (4) do (7), sta bili hitrost u_f in temperatura trdnine T_s zapisani kot dvodimenzionalno skalarno polje, medtem ko je bila temperatura tekočine T_f zapisana kot tridimenzionalno skalarno polje. Zaradi diskretizacijskega postopka je nastal, v primeru dvodimenzionalnih skalarnih polj, pet-diagonalni matrični sistem in, v primeru tridimenzionalnega skalarnega polja, sedem-diagonalni matrični sistem.

Za učinkovito obračanje matričnega sistema enačb je bila za ta poseben primer prizveta metoda spremenjenih vezanih gradientov (MSVG - PCGM), ki je podrobneje opisana v [11].

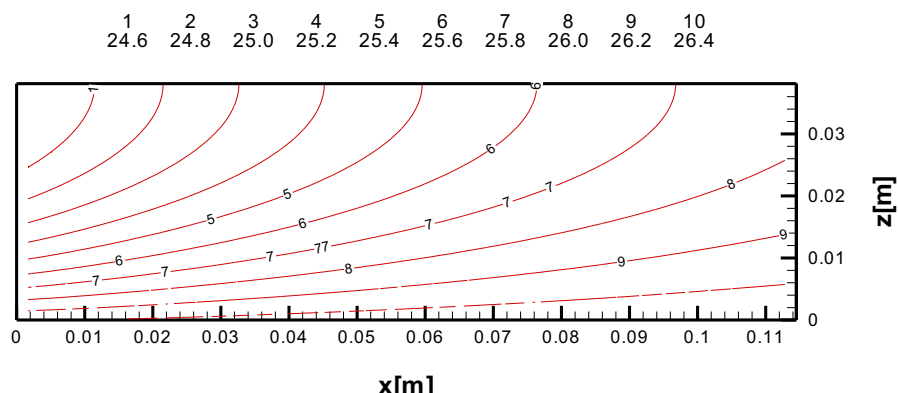
4 REZULTATI IN RAZPRAVA

Rezultati izračunov za primer aluminijastega (Al) hladilnika so predstavljeni na slikah 2 in 3. Tlačni padec $\Delta p = 368,6$ Pa povzroči zračni tok z Reynoldsovim številom $Re_h = 1904$, pri čemer je Reynoldsovo število definirano na podlagi hidravličnega premera d_h hipotetičnega kanala porozne snovi:

$$Re_h = \frac{\bar{u}_f d_h}{\nu_f} = \frac{\bar{u}_f}{\nu_f} \left(4 \frac{\alpha_f}{S} \right) \quad (8)$$

Slika 2 prikazuje temperaturno polje v Al strukturi v Celzijevi skali, medtem ko slika 3 razkriva temperaturno polje v zračnem toku.

Kakor prikazuje slika 2, ima Al struktura najvišjo temperaturo blizu izotermne spodnje stene in najnižjo temperaturo ob levem zgornjem robu, kjer je struktura izpostavljena vtoku zraka z nizko temperaturo. Slika 3 kaže, kako se zrak postopoma segreva od vtoka na levi do izzoda na desni strani. Spodnji del temperaturnega polja prav tako razkriva intenzivno segrevanje s spodnje izotermne meje, kar ima za posledico vodoravno topotno razslojenost prehajajočega zraka.



Sl. 2. Temperaturno polje v trdnini pri $Re_h = 1904$, $T_{in} = 22,85$ °C, $T_g = 26,64$ °C
Fig. 2. Temperature fields in the solid at $Re_h = 1904$, $T_{in} = 22.85$ °C, $T_g = 26.64$ °C

the principles of the finite-volume methods ([6] and [10]). In all the performed numerical simulations, $34 \times 17 \times 70$ finite volumes were used in x , y and z directions, respectively.

Due to the boundary conditions (4) to (7), the velocity u_f as well as the solid temperature T_s were described as two-dimensional scalar fields, whereas the fluid temperature T_f was described as a three-dimensional scalar field. This resulted in a non-symmetric five-diagonal matrix system for the two-dimensional scalar fields and a seven-diagonal matrix system for the three-dimensional scalar field.

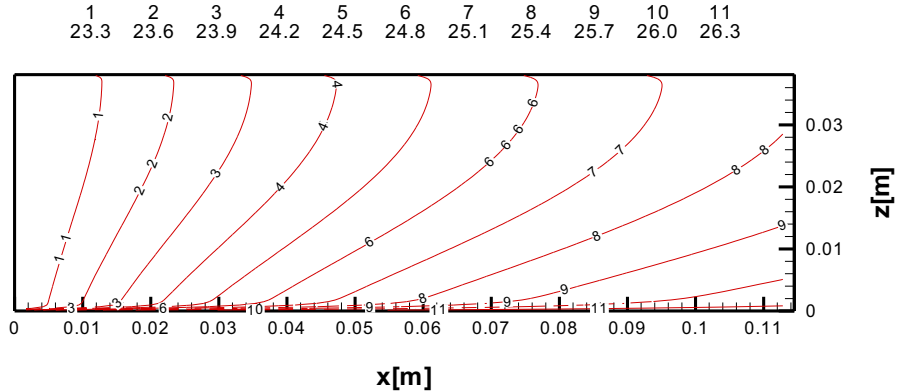
In order to invert the matrix systems efficiently, the preconditioned conjugate gradient method (PCGM), as described in [11], was adopted for this specific problem.

4 RESULTS AND DISCUSSION

The results of an example calculation for an aluminum (Al) heat sink are presented in Figs. 2 and 3. The imposed pressure drop $\Delta p = 368.6$ Pa causes airflow of the Reynolds number $Re_h = 1904$, where the definition of the Reynolds number is based on a hydraulic diameter d_h of a hypothetical porous media channel:

Fig. 2 shows the temperature field in the Al structure in degrees Celsius, whereas Fig. 3 reveals the temperature field in the airflow.

In Fig. 2, the Al structure has its highest temperature close to the isothermal bottom, and the lowest close to the left upper edge, where the structure is exposed to a low-temperature inflow. Fig. 3 shows how the air is gradually heated from the inlet on the left side to the outlet on the right side. The lower part of the temperature field also shows intensive heating from the isothermal bottom boundary, which results in horizontal thermal stratification of the passing air.



Sl. 3. Temperaturno polje v zraku pri $Re_h = 1904$, $T_{in} = 22,85^{\circ}\text{C}$, $T_g = 26,64^{\circ}\text{C}$
Fig. 3. Temperature fields in the air at $Re_h = 1904$, $T_{in} = 22.85^{\circ}\text{C}$, $T_g = 26.64^{\circ}\text{C}$

Poleg vzorčnega izračuna sta bili opravljeni še dve seriji izračunov pri osmih različnih tlačnih padcih. Pri izračunih uporabljeni robni pogoji so zbrani v preglednici 1. V obeh serijah smo za tok hladiva vzeli snovske lastnosti zraka. Pri prvi seriji izračunov smo za hladilnik vzeli snovske lastnosti aluminija, medtem ko je bila v drugi seriji predpostavljena izotermičnost strukture.

Kakor je običajno pri tovrstnih simuliranjih, sta bila izračunana koeficient upora \bar{C}_d (9) in Nusseltovo število \bar{Nu} (10) za celotno sekcijo, dobljene vrednosti pa primerjane z eksperimentalnimi rezultati [5].

$$\bar{C}_d = \frac{2 \Delta p}{\rho_f \bar{u}_f^2 L S} \quad (9),$$

$$\bar{Nu} = \frac{Q}{\Delta T A_g} \frac{d_h}{\lambda_f} \quad (10),$$

kjer sta: $A_g = L \cdot W$ površina gretega dna in $\Delta T = T_g - T_{in}$ temperaturna razlika med greto spodnjo steno in vtokom zraka. Pri definiciji Nusseltovega števila \bar{Nu} je konvektivni toplotni tok definiran kot:

$$\bar{Q} = \alpha_f \rho_f c_f \bar{u}_f \left(\bar{T}_{out} - \bar{T}_{in} \right) A_{\perp} \quad (11).$$

kjer je $A_{\perp} = H \cdot W$.

Primerjava na sliki 4 kaže koeficient upora celotne proge \bar{C}_d kot funkcijo Reynoldsovega števila Re_h . Slika kaže dobro ujemanje z že objavljenimi rezultati. Kljub temu pa se pri večji vrednosti Reynoldsovega števila Re_h zaradi naraščajoče turbulence, ki ni bila zajeta v model, pokaže razlika v velikosti nekaj odstotkov.

Primerjava porazdelitev Nusseltovega števila celotne proge \bar{Nu} na sliki 5 prikazuje večje odstopanje. Zaradi razlike v toplotnih robnih pogojih kažejo izračuni za 20 odstotkov večji toplotni tok od eksperimentalnih vrednosti [5]. Nadalje je razvidno, da končna toplotna prevodnost aluminijaste strukture (na slikah 5 in 6 označeno z Al) znižuje koeficient prestopa toplotne in Nusseltovo število \bar{Nu} v primerjavi s strukturo z neskončno toplotno

Besides the example calculation, two other series of calculations with eight different pressure drops were performed. The boundary conditions for these calculations are summarized in Table 1. In both series the air material properties were taken for coolant flow. For the first set of calculations the Al material properties were taken for the heat sink, whereas in the second set the heat sink was considered as isothermal.

As is usually the case in such calculations, the whole-section drag coefficient \bar{C}_d (9) and Nusselt number \bar{Nu} (10) were calculated and compared with the experimental results [5].

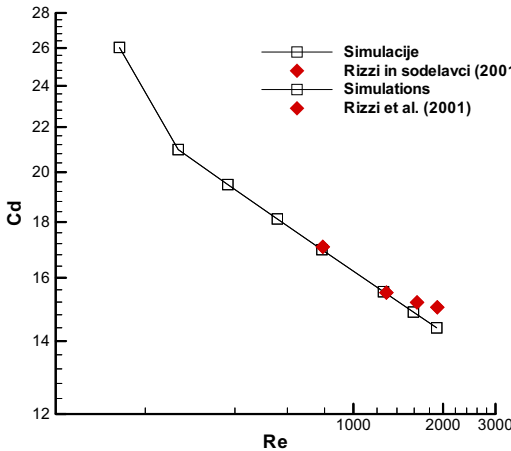
where $A_g = L \cdot W$ is the area of the heated bottom and $\Delta T = T_g - T_{in}$ is the temperature difference between the heated bottom and the inflow air. In the Nusselt number \bar{Nu} (10) definition, the convective heat-flow rate is defined as:

$$\bar{Q} = \alpha_f \rho_f c_f \bar{u}_f \left(\bar{T}_{out} - \bar{T}_{in} \right) A_{\perp} \quad (11).$$

where $A_{\perp} = H \cdot W$.

The comparison in Fig. 4 shows the whole-section drag coefficient \bar{C}_d as a function of Reynolds number Re_h . It reveals good agreement with already published data. Nevertheless, at a higher Reynolds number a difference of a few percent appears due to increasing turbulence, which was not taken into account in the model.

The comparison of the Nusselt number \bar{Nu} distributions in Fig. 5 shows larger discrepancies. Due to the difference in the thermal boundary conditions, the calculated data reveal up to 20 percent higher heat-transfer rate than the measured values [5]. Furthermore, it is evident that the finite thermal conductivity of the Al structure (in Figs. 5 and 6 marked with Al) decreases the heat-transfer coefficient and the Nusselt number \bar{Nu} in comparison



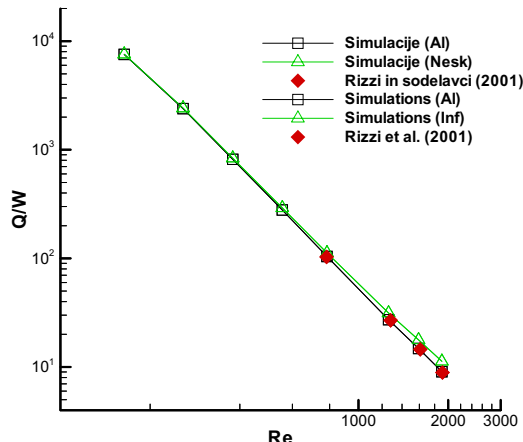
Sl. 4. Koeficient upora celotne sekcije kot funkcija Reynoldsovega števila
Fig. 4. Whole-section drag coefficient as a function of Reynolds number

prevodnostjo (na slikah 5 in 6 označeno z Nesk). Ta vpliv končne toplotne prevodnosti trdnine se z večanjem vrednosti Reynoldsovega števila še povečuje.

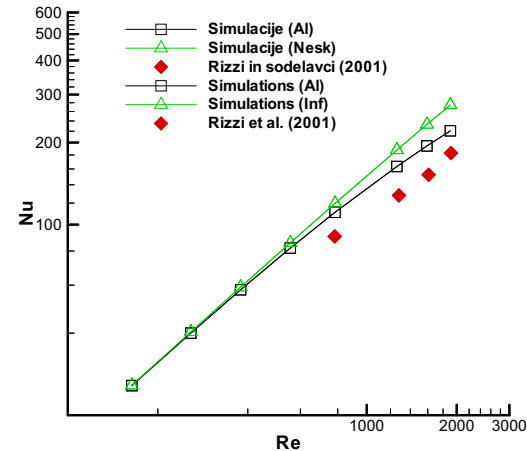
Konstrukcija prenosnikov toplote mora upoštevati tako vrednosti toplotnega toka kakor tudi mehanskega dela, ki je potrebno za premagovanje trenja tekočine in za premikanje le-te skozi samo strukturo. V tem pogledu je glavni cilj konstrukcije povečati toplotni tok \bar{Q} (11) pri najmanjši moči črpanja:

$$\bar{W} = \alpha_f \Delta p A_{\perp} \bar{u}_f \quad (12).$$

Slika 6 prikazuje toplotno učinkovitost prenosa toplote, ki je definirana kot razmerje med toplotnim tokom \bar{Q} in mehansko močjo \bar{W} . Razvidno je, da so eksperimentalni in numerični rezultati blizu skupaj. Pri padajoči toplotni učinkovitosti \bar{Q}/\bar{W} se vpliv toplotne prevodnosti poveča in povzroči 35 odstotkov razlike pri vrednosti Reynoldsovega števila $Re_h = 1904$.



Sl. 6. Topotna učinkovitost hladilnika v odvisnosti od Reynoldsovega števila
Fig. 6. Heat-sink effectiveness as a function of Reynolds number



Sl. 5. Nusseltovo število celotne sekcije kot funkcija Reynoldsovega števila
Fig. 5. Whole-section Nusselt number as a function of Reynolds number

with the infinite thermal conductivity case (in Figs. 5 and 6 marked with Inf). This influence of finite thermal conductivity of the solid becomes larger with increasing Reynolds number.

The design of a heat sink involves consideration of the heat-transfer rate and the mechanical pumping power expended to overcome fluid friction and move the fluid through a structure. Thus, the main design goal is to maximize the heat-transfer rate \bar{Q} (11) for the minimum pumping power:

Fig. 6 shows the thermal effectiveness of the heat-transfer process, which is defined as the ratio between the heat-transfer rate \bar{Q} and the mechanical power \bar{W} . It is evident that the experimental and numerical results are close. With decreasing thermal effectiveness \bar{Q}/\bar{W} , the influence of the structure's thermal conductivity increases and causes a 35 percent difference at the Reynolds number $Re_h = 1904$.

Kakor je prikazano, se toplotna učinkovitost \bar{Q}/\bar{W} hladilnika zmanjšuje z večanjem vrednosti Reynoldsovega števila Re_h (8). Kljub temu, da manjše vrednosti Reynoldsovega števila Re_h prinašajo večjo toplotno učinkovitost, pa morajo biti rezultirajoči majhni toplotni tokovi nadomeščeni z večjo površino in zaradi tega z večjimi dimenzijskimi samega hladilnika. V nekaterih primerih to ni mogoče zaradi gospodarnosti in omejitve velikosti.

5 SKLEPI

Prispevek opisuje delo, ki je bilo vloženo v razvoj računskega hitrega numeričnega algoritma za izračun prenosnikov toplotne. Namen naloge je bil posvečen numerični raziskavi odvoda toplotne iz elektronskega čipa. Pri tem je bila notranja struktura hladilnika, v obliki paličastih reber s premaknjeno postavitvijo, obravnavana kot homogena porozna snov. Vrednosti koeficientov lokalnega upora C_d in prestopa toplotne h , ki so bile potrebne za zaprtje prenosnih enačb, smo prevzeli iz [7] do [9]. Razvite parcialne diferencialne enačbe so bile diskretizirane z upoštevanjem ohranitvenih lastnosti metode nadzornih prostornin. Sistem pol-linearnih enačb je bil nato rešen z metodo spremenjenih vezanih gradientov. Za preveritev postopka izračuna smo uporabili eksperimentalne podatke laboratorija za prenos toplotne "Morrin-Martinelli-Gier".

Izvedeni sta bili dve seriji izračunov za hladilnik čipa, ki je bil hlajen z zračnim tokom. Izračunane vrednosti koeficiente upora celotne proge \bar{C}_d kažejo dobro ujemanje z že objavljenimi podatki, medtem ko izračunane vrednosti Nusseltovega števila \bar{Nu} celotne proge razkrivajo odstopanje zaradi razlik v toplotnih robnih pogojih. Prav tako smo raziskali vpliv končne toplotne prevodnosti trdne strukture. Izkazalo se je, da končna toplotna prevodnost aluminija zmanjša toplotno učinkovitost \bar{Q}/\bar{W} za 35 odstotkov pri $Re_h = 1904$. Prav tako je pričakovati večji vpliv toplotne prevodnosti pri večjih vrednostih Reynoldsovega števila.

Prikazani rezultati potrjujejo ustreznost izbranega načina za preračun hladilnika, kjer je treba upoštevati toplotno prevodnost trdne strukture. Vzorčni izračuni prav tako potrjujejo, da razvit numerični program daje rezultate z zadostno natančnostjo za razširitev njegove uporabe na druge bolj zahtevne geometrijske oblike.

Zahvala

Prvi avtor se želi zahvaliti za finančno podporo skladu Kerze-Cheyovich in Ministrstvu za šolstvo, znanost in šport Republike Slovenije.

The thermal effectiveness \bar{Q}/\bar{W} of the examined heat sink is reduced with increasing Reynolds number Re_h . Although the lower Reynolds numbers Re_h bring higher effectiveness, the resulting low-heat-transfer rates have to be compensated with a larger heat-transfer surface and consequently with a larger heat sink. In some cases this is not possible due to economics and size limitations.

5 CONCLUSIONS

The present paper describes an effort to develop a fast-running numerical algorithm for heat-exchanger calculations. The purpose of the task was to numerically investigate heat removal from an electronic chip. The heat sink's internal structure, in the form of a staggered arrangement of pin-fins, was treated as a homogenous porous media. The local values of drag coefficient C_d and heat-transfer coefficient h , which were needed to close the transport equations, were taken from [7] to [9]. The resulting partial differential equations were discretized using conservation properties of the finite-volume method. The system of semi-linear equations was solved with the preconditioned conjugate gradient method. To test the calculation procedure, experimental data obtained in the Morrin-Martinelli-Gier Memorial Heat Transfer Laboratory were used for the comparison.

Two series of calculations were performed for the heat sink cooled with airflow. The calculated values of the whole-section drag coefficient \bar{C}_d show a good agreement with already published data, whereas the calculated whole-section values of the Nusselt number \bar{Nu} reveal some discrepancies due to differences in the thermal boundary conditions. Also, the influence of the finite thermal conductivity of the solid structure was examined. It was shown that the finite thermal conductivity of aluminum decreases the thermal effectiveness \bar{Q}/\bar{W} by 35 percent at $Re_h = 1904$. Furthermore, it is expected that at a higher Reynolds number this thermal conductivity effect would increase.

The presented results demonstrate that this approach is appropriate for heat-sink calculations where the thermal conductivity of a solid structure has to be taken into account. The example calculations also verify that the developed numerical code yields sufficiently accurate results to be also applicable for other more demanding geometries.

Acknowledgements

The first author's financial support by the Kerze-Cheyovich scholarship and the Ministry of Education, Science and Sport of the Republic of Slovenia is gratefully acknowledged.

6 LITERATURA
6 REFERENCES

- [1] Hesselgreaves, J.E. (2001) Compact heat exchangers selection, *Design and Operation, Pergamon Press*.
- [2] Whitaker, S. (1967) Diffusion and dispersion in porous media, *AICHE Journal*, Vol. 13, No. 3, 420-427.
- [3] Travkin, V.S., I. Catton (1995) A two temperature model for fluid flow and heat transfer in a porous layer, *J. Fluid Engineering*, Vol. 117, 181-188.
- [4] Travkin, V.S., I. Catton (1999) Transport phenomena in heterogeneous media based on volume averaging theory, *Advans. Heat Transfer*, Vol. 34, 1-143.
- [5] Rizzi, M., Canino, M., Hu, K., Jones, S., Travkin, V., Catton, I. (2001) Experimental investigation of pin fin heat sink effectiveness, *Procs. of the 35th National Heat Transfer Conference*, Anaheim, California.
- [6] Horvat, A., I. Catton (2001) Development of an integral computer code for simulation of heat exchangers, *Procs. of the Conf. "Nuclear Energy in Central Europe 2001"*, Portorož, Slovenia, Sept. 10-13, No. 213.
- [7] Launder, B.E., T.H. Massey (1978) The numerical prediction of viscous flow and heat transfer in tube bank. *Trans, ASME J. Heat Transfer*, Vol. 100, 565-571.
- [8] Kays, W.M., A.L. London (1998) Compact heat exchangers, 3rd Ed. *Krieger Publishing Company*, Malabar, Florida, 146-147.
- [9] Žukauskas, A.A., R. Ulinskas (1985) Efficiency parameters for heat transfer in tube banks, *J. Heat Transfer Engineering*, Vol.5, No.1, 19-25.
- [10] Versteeg, H.K., W. Malalasekera (1995) An introduction to computational fluid dynamics, The Finite Volume Method, *Longman Scientific & Technical: England*, 103-1335.
- [11] Ferziger, J.H., M. Perić (1996) Computational method for fluid mechanics, Chapter 5: Solution of linear equation systems, *Springer Verlag: Berlin*, 85-127.

Naslova avtorjev:

dr. Andrej Horvat
Odsek za reaktorsko tehniko
Institut "Jožef Stefan"
Jamova 39
1111 Ljubljana

prof.dr. Ivan Catton
Morrin-Martinelli-Gier Memorial Heat
Transfer Laboratory
Department of Mechanical and Aerospace
Engineering
School of Engineering and Applied Science
University of California, Los Angeles
420 Westwood Plaza, Eng. IV, 90095
Los Angeles, California, USA

Author's Addresses:

Dr. Andrej Horvat
Reactor Engineering Division
Institute "Jožef Stefan"
Jamova 39
SI-1111 Ljubljana, Slovenia

Prof.Dr. Ivan Catton
Morrin-Martinelli-Gier Memorial Heat
Transfer Laboratory
Department of Mechanical and Aerospace
Engineering
School of Engineering and Applied Science
University of California, Los Angeles
420 Westwood Plaza, Eng. IV, 90095
Los Angeles, California, USA

Prejeto:
Received: 6.5.2002

Sprejeto:
Accepted: 22.11.2002